Engineering Science and Technology, an International Journal 19 (2016) 1600–1607

HOSTED BY

Contents lists available at ScienceDirect

Engineering Science and Technology, an International Journal

journal homepage: www.elsevier.com/locate/jestch

Full Length Article

Wind-driven SEIG supplying DC microgrid through a single-stage power converter

Vellapatchi Nayanar, Natarajan Kumaresan *, Nanjappa Gounder Ammasai Gounden

National Institute of Technology, Tiruchirappalli, Tamil Nadu 620 015, India

ARTICLE INFO

Article history:
Received 21 February 2016
Revised 3 May 2016
Accepted 30 May 2016
Available online 8 June 2016

Keywords:
DC microgrid
Digital signal controller (DSC)
Induction generators
Maximum power point tracking (MPPT)
Semi-converter
Wind energy conversion system (WECS)

ABSTRACT

Nowadays, there is an increased emphasis on utilizing the renewable energy sources and selection of suitable power converters for supplying dc microgrid. Among the various renewable energy sources, wind energy stands first in terms of installed capacity. So, an attempt is made in this paper for supplying dc microgrid utilizing wind energy. A self-excited induction generator has been used in the proposed wind energy conversion system (WECS). A single-stage power converter, namely, semi-converter is connected between the SEIG and dc grid terminals for closed-loop control of the proposed system. A perturb and observe (P&O) based maximum power point tracking (MPPT) algorithm has been developed and implemented using a dsPIC30F4011 digital controller. In this MPPT algorithm, the firing angle of the converter is adjusted by continuously monitoring the dc grid current for a given wind velocity. For analyzing the proposed system, a MATLAB/Simulink model has been developed by selecting the various components starting from wind-turbine model to the power converter supplying dc microgrid. Successful working of the proposed WECS has also been shown through experimental results obtained on a prototype model developed in the laboratory.

1. Introduction

In the past decades, there is a substantial increase in the installed capacity of the wind power plants to meet out the growing power demand and also to have the pollution free environment [1–5]. In such systems, squirrel-cage induction machines functioning as generators are being used due to their low cost, simple, robust construction and almost nil maintenance requirements [5–12]. This machine can be operated either as a grid-connected induction generator for supplying power to the grid or self-excited induction generator (SEIG) for feeding power to the isolated loads.

It is known that the operating slip and hence rotational speed of the induction generator directly feeding power to the grid will have a very small variation from no load to full load [13,14]. However, for extracting the maximum power (MP) available in the wind by operating the wind turbine with optimum power coefficient, this rotational speed should be allowed to vary widely. For achieving this, the machine has been operated in self-excited mode with capacitors connected at the stator terminals [13–17]. Then, suitable power converter needs to be interfaced between the generator terminals and ac grid. Various control strategies have also been proposed in the literature for controlling these power converters for extracting MP available in the wind and feed to the ac grid [13–17]. Fast and exact detection of phase and frequency of grid voltage/current is needed to control the power converters in wind-generator systems [18]. Further, the intermittent nature of wind power output would affect the operation of interconnected systems as well as the grid side power quality [19]. So, integration of the energy storage devices is proposed in the literature to smooth out this fluctuating power output from wind [20–23].

With the development of power electronic technologies and increased use of distributed generators (DGs) with renewable energy, hybrid ac/dc microgrid has been proposed in the literatures for providing more green and high quality energy with the highest efficiency [24,25]. Main advantage of hybrid ac/dc microgrid is the elimination of unnecessary multi-conversion stages which reduces the total conversion loss and cost reduction in electronic products. Increased use of dc loads such as LED lighting, computer loads, electric vehicles and variable speed drives is inevitable and such loads are connected to dc micro grids with reduced power converter stages [26–30]. Fig. 1 shows the typical structure of the

* Corresponding author at: Department of Electrical and Electronics Engineering, National Institute of Technology, Tiruchirappalli, Tamil Nadu 620 015, India.
E-mail addresses: vnayanar27@gmail.com (V. Nayanar), nkumar@nitt.edu (N. Kumaresan), amms@nitt.edu (N.G. Ammasai Gounden).

Peer review under responsibility of Karabuk University.

http://dx.doi.org/10.1016/j.jestch.2016.05.016
2215-0986/

Nomenclature

List of abbreviations:

DSC	digital signal controller
MPPT	maximum power point tracking
P&O	perturb and observe
SEIG	self-excited induction generator
WECS	wind energy conversion systems
WT	wind-turbine
ZCD	zero crossing detector

List of symbols:

C	excitation capacitance per phase, F
f_g	generated frequency, Hz
I_C	capacitor line current, A
I_{dc}	dc grid current, A
I_R	rectifier input line current, A
I_S	stator line current, A
N_r	actual rotor speed, rpm
P_{dc}	dc grid power, W
P_e	electrical output power from the generator, W
P_m	WT output power/mechanical input power to the generator, W
V_{dc}	dc grid voltage, V
V_S	line voltage at the generator terminals, V
V_w	wind velocity, m/s
α	firing angle, degree

low/medium voltage dc microgrid system. DC microgrid also helps in effective coordination among DGs so that the power balance is maintained between source and load. As an example, Strunz et al. have proposed a dc microgrid system for harnessing wind and solar energy that occur at the top of high-raised buildings [31]. Present authors have recently proposed a two-stage power converter, namely, diode bridge rectifier and dc–dc converter for feeding power to a 120 V dc microgrid from wind-driven SEIG [32].

The objective of the present work is to employ a single stage power converter, namely, three-phase semi-converter, for supplying 120 V dc microgrid from wind-driven SEIG. As only one quadrant operation is required in wind energy conversion systems i.e., power flow is always from SEIG terminals to the dc grid, a three-phase semi-converter circuit would suffice for such application. Further, semi-converter requires less number of control devices i.e., thyristors and firing circuits as compared to full converter to achieve the same operation. As the dc grid voltage is held constant at 120 V, any variation in the wind power output will reflect in the variation of dc grid current. Hence, dc grid current is continuously monitored for tracking the MP available in the wind by appropriately adjusting the firing angle of the semi-converter in closed-loop operation. In this work, perturb and observe (P&O) based maximum power point tracking (MPPT) algorithm has been developed by sensing this dc grid current for any given wind velocity. The proposed algorithm is free from machine parameters as it uses only the measured value of electrical parameters and hence it is simple to implement. A MATLAB simulation model has been developed to ascertain the successful working of the proposed system and closed-loop algorithm for MPPT. The efficacy of the system has also been demonstrated with the results obtained from the experimental set-up.

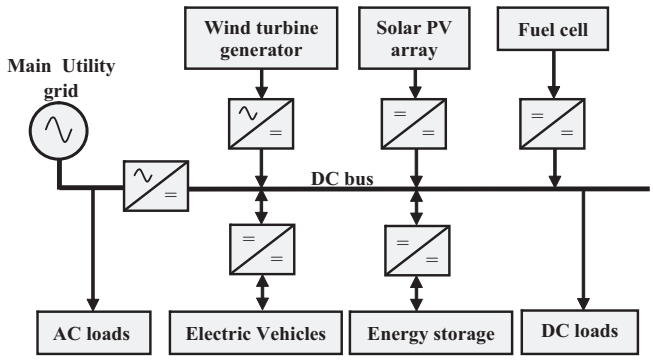

Fig. 1. Structure of low/medium voltage dc microgrid.

The description of the proposed WECS employing SEIG and semi-converter is given in Section 2. The MPPT algorithm and generation of synchronized triggering pulses for the operation of three-phase semi-converter are also presented in the same section. Analysis of proposed system using MATLAB/Simulink model, simulation results and discussions are given in Section 3. Hardware details of the proposed system and results obtained on the prototype model developed in the laboratory are furnished in Sections 4 and 5 brings out the major conclusions.

2. Description of the proposed DC microgrid system

Fig. 2 shows the proposed wind energy conversion system (WECS) feeding dc microgrid. This system consists of a wind-driven SEIG and thyristor based three-phase semi-converter with appropriate firing and control circuits. A 120 V dc microgrid is considered for operating the proposed system [32]. A smoothing inductor is connected in between the output side of semi-converter and dc microgrid to have the continuous dc grid current. In the case of SEIG, the output voltage and frequency vary with the driving speed and load [5–14]. For the present system, this variable voltage and variable frequency (VVVF) output from SEIG is fed to the three-phase semi-converter. For balanced operation of semi-converter (i.e., triggering the thyristors at 120° interval), it is necessary to sense this VVVF signal through appropriate transducers and feed it to the zero crossing detector (ZCD) circuits. ZCD output is fed to the controller which calculates the frequency and identifies the voltage zero crossing point for generating the firing pulses to trigger the thyristors.

The MPPT algorithm proposed in this work assumes that the dc grid voltage is stiff and constant at 120 V. This leads to the variation in the dc grid current for any change in the SEIG output power due to the variation in the wind velocity. So, the proposed algorithm continuously monitors the value of dc grid current for tracking the MP available in the wind. MPPT has been realized using P&O algorithm. It involves the comparison of the present and previous values of the dc grid current. The relative value of this comparison decides the adjustment of the firing angle, α for tracking MP available in the wind as described in the flowchart of Fig. 3. Further, it is known that the WT should be made to operate with specific rotational speed for a given wind velocity to extract MP available in the wind [15–17,32]. This has been achieved in this work by adjusting the firing angle of the power converter for any wind velocity.

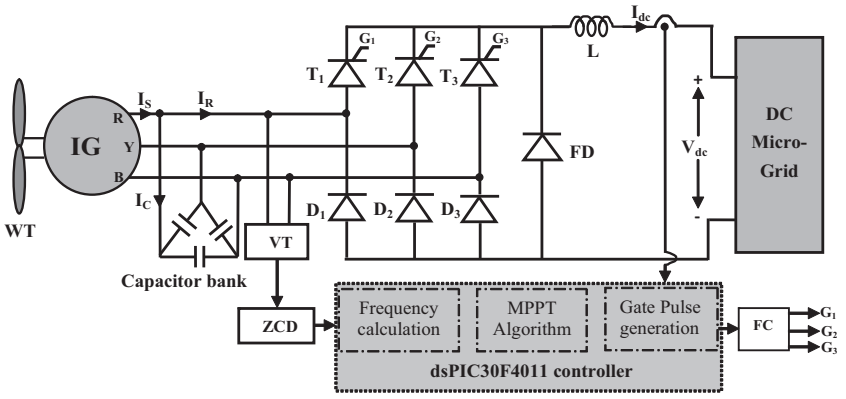

Fig. 2. Schematic diagram of the proposed wind-driven SEIG-Converter system for dc microgrid applications. WT: wind turbine; IG: induction generator; VT: voltage transducer; ZCD: zero crossing detector; FD: freewheeling diode and FC: firing circuits.

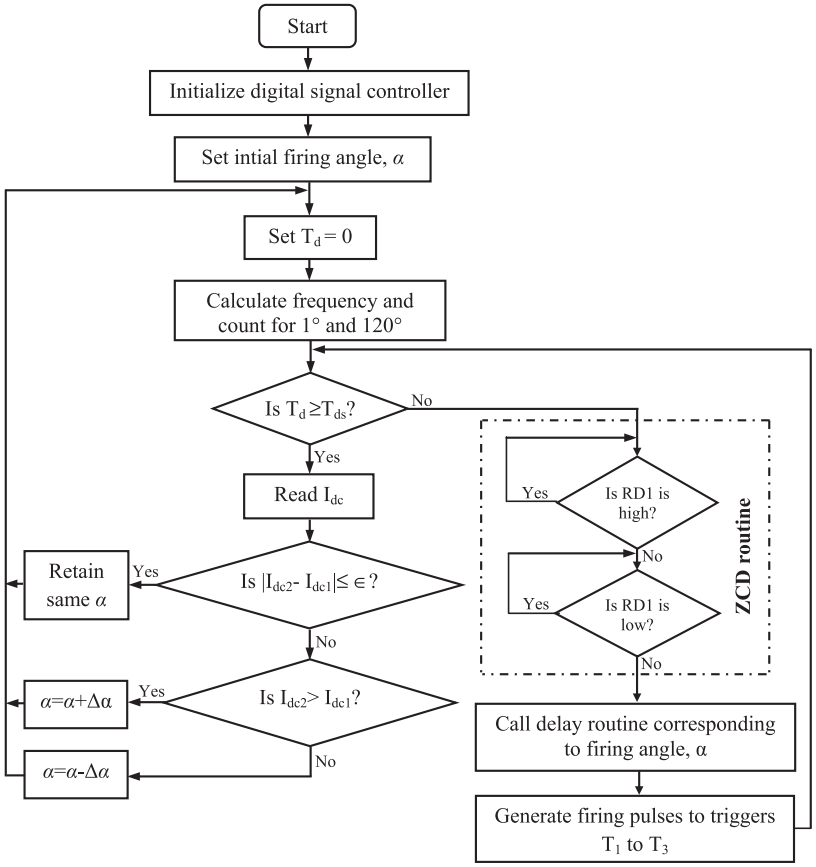

Fig. 3. Flowchart for the MPPT algorithm for wind-driven SEIG system. ZCD: zero crossing detector and ZCD output is given to the IC2/PD1 (Port D) of dsPIC30F4011 digital controller; ∈: tolerance; ∝: firing angle; I_{dc}: dc grid current; I_{dc1}: previous dc grid current; I_{dc2}: present dc grid current and T_{ds}: delay time (0.1 s).

3. Analysis of the proposed WECS

A three-phase, four-pole, 230 V, 50 Hz (1 p.u. frequency), 3.7 kW, delta-connected squirrel-cage induction machine has been considered for the analysis of the proposed WECS. A delta connected capacitor bank of 100-μF per phase has been chosen for operating the induction machine in self-excited mode [8,10,13]. For this value of capacitance, the machine delivers its rated power with a voltage of 230 V at rated speed of 1500 rpm (1 p.u. speed). The measured parameters of the induction machine are

Table 1
No-load saturation characteristic of a three-phase, four-pole, 230 V, 50 Hz, 3.7 kW, delta-connected squirrel-cage induction machine at rated speed of 1500 rpm.

I (A)	1.7	2.6	3.3	3.8	4.3	6.1	8.1	10.5	11.5	14.1	16.2	18.0
V (V)	118	163	190	208	223	255	285	300	321	367	386	395

$R_1 = 1.30\ \Omega$, $R_2 = 1.75\ \Omega$ and $X_1 = X_2 = 2.6\ \Omega$. Experimentally obtained magnetization characteristic of the induction machine at rated speed and frequency is given in Table 1. To demonstrate the working of the proposed WECS for feeding dc microgrid, the system shown in Fig. 2 has been simulated using SimPowerSystems toolbox in MATLAB. The above measured parameters of the induction machine along with the magnetization characteristic are used in the simulation and the details are described in the succeeding sub-sections:

3.1. Simulation model

The machine parameters along with the magnetization characteristic have been inserted in the asynchronous machine model available in the MATLAB for analyzing the working of proposed system. A three-phase semi-converter has been built using the thyristor and diode models available in the MATLAB. The output terminals of the asynchronous machine model operating as SEIG is connected to the ac terminals of the semi-converter. The dc terminals of the converter are connected to the 120 V dc bus/microgrid through a 50 mH smoothing inductor. For this simulation, dc microgrid has been realized by using the generic battery model available in the MATLAB/SimPowerSystems toolbox. Dynamic modeling of the WT for driving the SEIG is implemented with the following set of equations [15–17]:

The mechanical output power of the WT, P_{WT} is given by:

$$P_{WT} = \frac{1}{2} C_p(\lambda,\ \beta)\rho A V_w^3 \tag{1}$$

where ρ is the air density in kg/m^3, A is the swept area (πR^2) in m^2 by the turbine blades, R is the radius of the blade in m, V_w is the wind velocity in m/s and WT power coefficient C_p (λ, β) is given by:

$$C_p(\lambda,\ \beta) = c_1\left(\frac{c_2}{\lambda_i} - c_3\beta - c_4\right)e^{\frac{-c_5}{\lambda_i}} + c_6\lambda \tag{2}$$

and

$$\frac{1}{\lambda_i} = \frac{1}{\lambda + 0.08\beta} - \frac{0.035}{\beta^3 + 1} \tag{3}$$

The coefficients c_1 to c_6 are: $c_1 = 0.5176$, $c_2 = 116$, $c_3 = 0.4$, $c_4 = 5$, $c_5 = 21$ and $c_6 = 0.0068$.

Tip speed ratio, λ is expressed as:

$$\lambda = R\omega_r/V_w \tag{4}$$

where ω_r is the rotational speed of the WT in rad/s.

The mechanical torque produced by the WT can be expressed as:

$$T_m = P_{WT}/\omega_r \tag{5}$$

Following parameters have been chosen for driving the 3.7 kW SEIG: nominal mechanical output power, $P_m = 5$ kW; base wind velocity, $V_w = 12$ m/s; maximum power at base wind velocity = 0.95 p.u.; base rotational speed = 1 p.u. (= 1500 rpm); gear ratio = 1:1, $\rho = 1.205$ kg/m^3; C_p (max) = 0.48 for $\lambda = 8.1$ and $\beta = 0°$. The mechanical power output and the corresponding rotational speed of the WT at MPPT condition calculated using these values and (1)–(5) are given in Table 2 for the typical wind velocities. It is to be noted that the WT model available in the MATLAB gives the mechanical torque as output for a given wind velocity. So, negative value of this torque is given as input to the asynchronous machine model for SEIG operation.

Table 2
Mechanical output power and corresponding rotational speed of WT at MPPT condition.

S. No	Wind velocity (V_w), m/s	Rotational speed (N_r), rpm	WT maximum output power (P_m), kW
1.	8	1140	1.22
2.	9	1225	1.76
3.	10	1336	2.42
4.	11	1421	3.21
5.	12	1500	4.19

The algorithm given in the flowchart of Fig. 3 has been coded using the embedded MATLAB function for the closed-loop operation of the proposed system. This function receives ZCD and dc grid current signals and gives the appropriate firing pulses to the semi-converter to extract MP available in the wind. This closed-loop control of semi-converter will operate the WT with rotational speed and output power for any given wind velocity as per the typical values mentioned in Table 2 for MPPT.

3.2. Simulation results

Firstly, simulation has been carried out for the steady-state analysis of the proposed system for a given wind velocity and results are given in Fig. 4 for extracting the MP available in the wind. In this simulation, firing angle is adjusted by monitoring the dc grid current as per the logic described in the flowchart of Fig. 3. It has been observed from the simulation that the rotational speed of the WT and the corresponding mechanical power output automatically reach the specific values as per the WT characteristics mentioned in Table 2 for MPPT operation. Thus, the simulated results given in Fig. 4 validate the successful working of the proposed WECS for feeding dc microgrid and the closed-loop operation of MPPT algorithm.

The system has also been simulated for step change in wind velocity to illustrate the successful tracking of the MP point employing the proposed MPPT algorithm. Simulated results for step change in wind velocity from 8 to 10 m/s and back are provided in Fig. 5. This figure gives the simulated waveforms of rotor speed (N_r), mechanical torque of the WT (T_m), electromagnetic torque (T_e) of generator, stator output power (P_e), stator voltage (v_S), stator current (i_S), capacitor current (i_C), rectifier input current (i_R), dc grid current (I_{dc}) and dc grid power (P_{dc}). As mentioned earlier T_m & T_e are given negative values for operating the asynchronous induction machine as a SEIG. It can be seen from this figure that the closed loop controller adjusts the firing angle by continuously monitoring the dc grid current so that the rotational speed and mechanical power output settle at the specified value for MPPT as given in Table 2. As an example, the firing angle is adjusted to 97° by closed-loop control with a dc grid current of 15.1 A, which settles the rotational speed at 1332 rpm with the mechanical output power of 2.42 kW under steady-state for a wind velocity of 10 m/s.

4. Experimental verification

A prototype model has been built in the laboratory to illustrate the closed-loop operation of the proposed WECS supplying dc microgrid. The same three-phase, four-pole, 230 V, 3.7 kW SEIG with a capacitance of 100 μF per phase used for the analysis of the proposed system in the previous section, has been considered for the experimental investigations. In the laboratory set-up, wind turbine has been emulated with a separately excited dc motor for driving the SEIG. A three-phase semi-converter has been built using International Rectifier make thyristors (50RIA120) and Ruttonsha Associate make power diodes (70HMR100) along with the appropriate firing circuits. A 10-kVA online solar inverter system (Emerson make – Liebert ESU model) has been used for realizing dc microgrid. It consists of (i) solar-photovoltaic arrays with

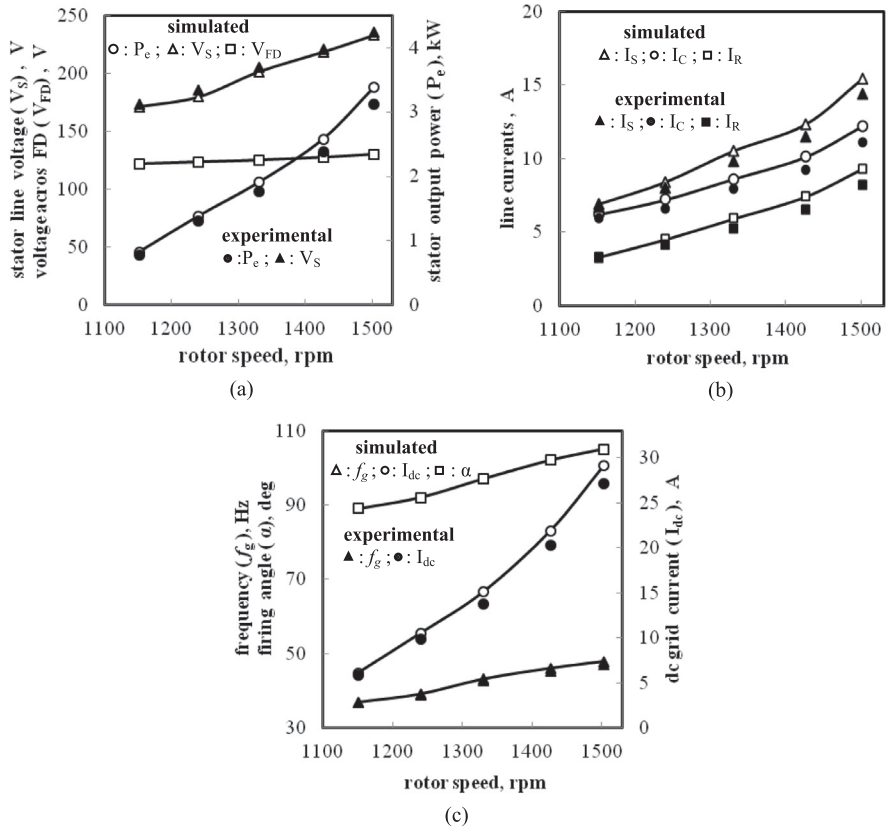

Fig. 4. Performance of the SEIG system operating in MP condition for various rotor speeds. (a) Variation of stator line voltage, voltage across FD, stator output power against rotor speed. (b) Variation of stator line current (I_S), capacitor line current (I_C), rectifier input line current (I_R) against rotor speed. (c) Variation of generator frequency, dc grid current, firing angle against rotor speed.

dc–dc converter, (ii) battery banks and (iii) bidirectional converter i.e., IGBT based voltage source inverter. All power electronic converters are connected to a common dc bus, which forms dc microgrid for the experimental setup. This dc microgrid voltage is maintained at 120 V (within ±5%) by the closed-loop controller present in the unit.

A 16-bit dsPIC30F4011 digital signal controller (DSC) operates with the specified frequency that can be obtained by either internal RC oscillator or external crystal oscillator with the on-chip phase locked loop (PLL) based timer prescaler value. Further, the PLL is selectable to have the prescaler (PR) gains of 4, 8 and 16. In the present case, the operating frequency (F_O) of dsPIC30F4011 is calculated in terms of million instructions per second (MIPS) by using $F_O = (F_{OSC} \times PR)/4$. For the present work, 10 MHz ($= F_{OSC}$) crystal oscillator has been used and PLL prescaler value is taken as 8 so that $F_O = 20$ MIPS. This is achieved by writing appropriate embedded-C program into dsPIC30F4011 DSC. Further, it contains 10-bit analog to digital converter (ADC) with nine numbers of analog input channels which has been used for developing the closed-loop control algorithm described in Section 2. A LEM make current transducer (LA 55-P) has been used for sensing the dc grid current of the converter. The output obtained from the current sensor through signal conditioning circuit has been given as input to one of the ADC channels available in DSC (AN2 in Port B) for developing MPPT control algorithm.

The line voltage of the induction generator is sensed using a LEM make voltage transducer (LV 25-P) for calculating the frequency and identifying the zero crossing point of the voltage. This is essential for generating the synchronized firing/triggering pulses, since the frequency of the output voltage from SEIG will vary with wind velocity. The output of voltage transducer is given to the op-amp based ZCD circuit shown in Fig. 6. The output of ZCD waveform is given as input to one of the input capture module available in the DSC (IC2 in Port D). The time interval between two rising edge of ZCD waveform has been calculated to evaluate the value of the generator frequency. Further, the rising edge of ZCD waveform has been used as reference point for generating firing angle, α. The sequence for generating synchronized firing/triggering pulses are also given in the flowchart of Fig. 3. These pulses are taken out from port E (RE0, RE2 and RE4) of DSC and given to the thyristors through firing circuits.

To show the working of the prototype system developed in the laboratory, experiments have been conducted by setting different rotor speeds with the corresponding firing angle given in Fig. 4c corresponding to the MPPT condition for a given wind velocity. Various performance quantities have been observed for these operating points and these experimental results are also given in Fig. 4. The waveforms of the stator voltage, stator current, capacitor current and converter input current were also observed using Digital Storage Oscilloscope (DSO) for different rotor speeds with the firing angle corresponding to MPPT conditions. For the sake of brevity, experimentally obtained waveforms stored using DSO for two operating points (corresponding to 8 and 10 m/s) are given in Fig. 7. A close agreement between the simulated and experimental results given in Fig. 4 and also the waveforms given in Figs. 5 and 7, validates the practical implementation of the proposed WECS for supplying dc microgrid.

The SEIG will give one value of MP for the given rotor speed and excitation capacitor [13,32]. As an example, the experimental machine considered in this work will give a maximum power of

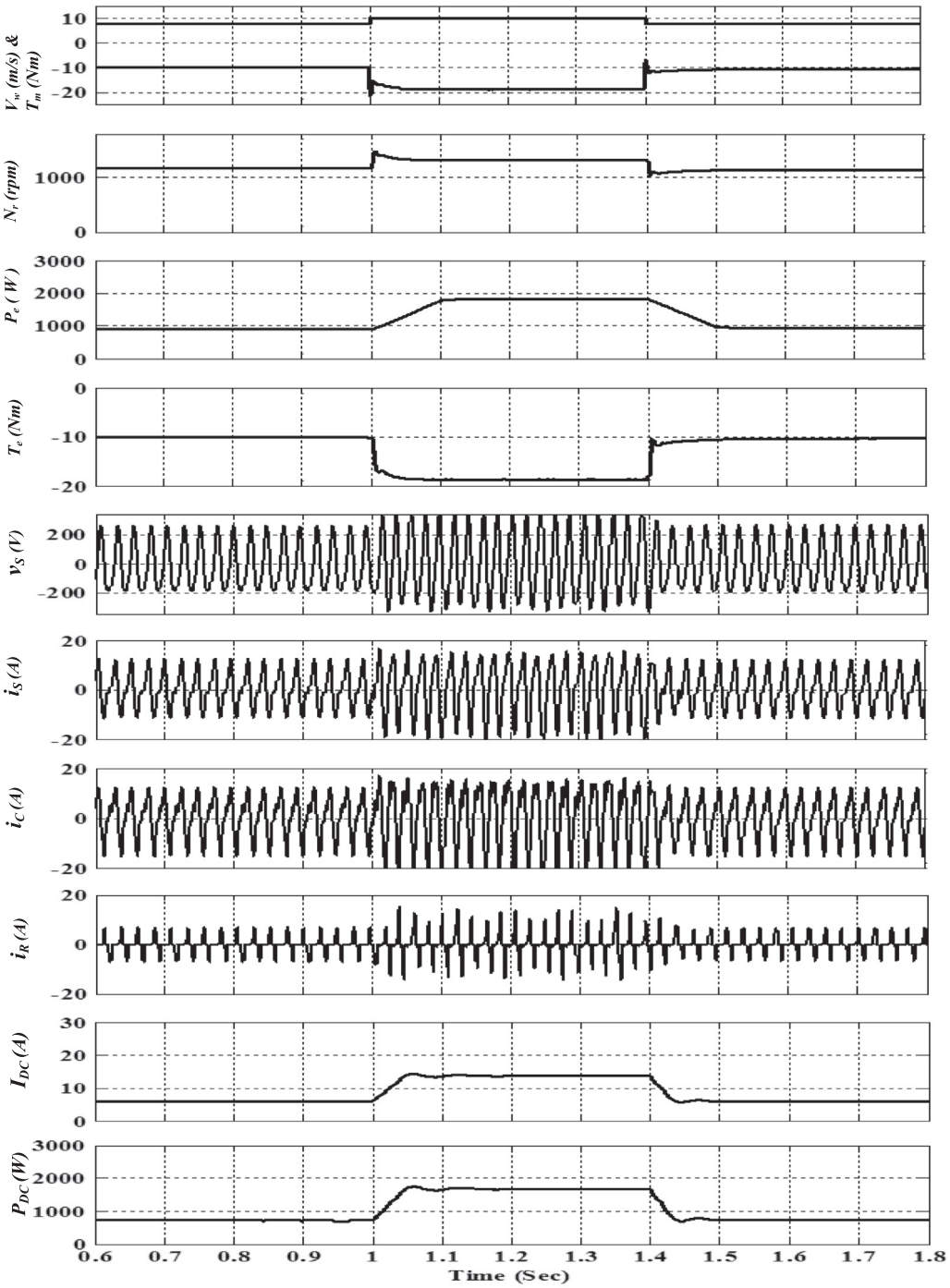

Fig. 5. Dynamic response of the proposed WECS for step change in wind velocity from 8 to 10 m/s at $t = 1$ s and 10 to 8 m/s at $t = 1.4$ s. $V_{dc} = 120$ V.

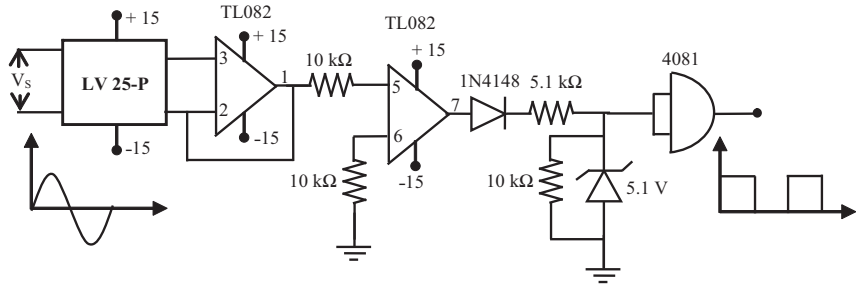

Fig. 6. Op-amp based zero-crossing detector circuit.

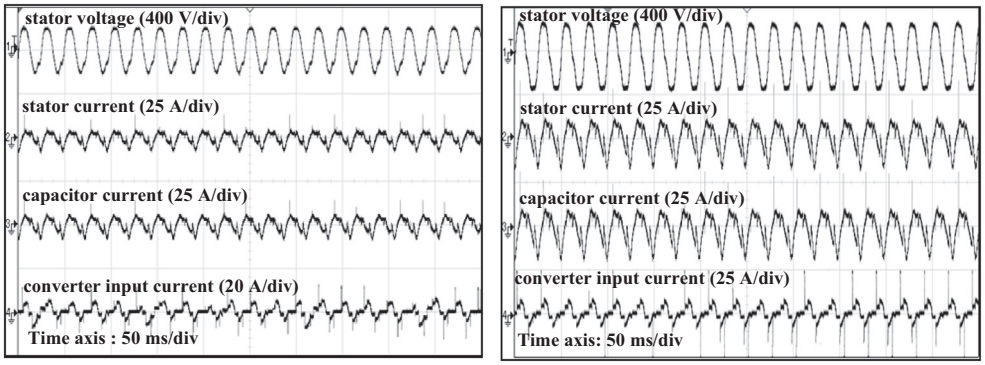

(a) 1140 rpm (corresponding to 8 m/s) (b) 1332 rpm (corresponding to 10 m/s)

Fig. 7. Performance of the proposed system at MPPT condition for wind velocities of 8 and 10 m/s. V_{dc} = 120 V, I_{dc} = 6.1 A & α = 89° for 8 m/s and I_{dc} = 13.6 A & α = 97° for 10 m/s.

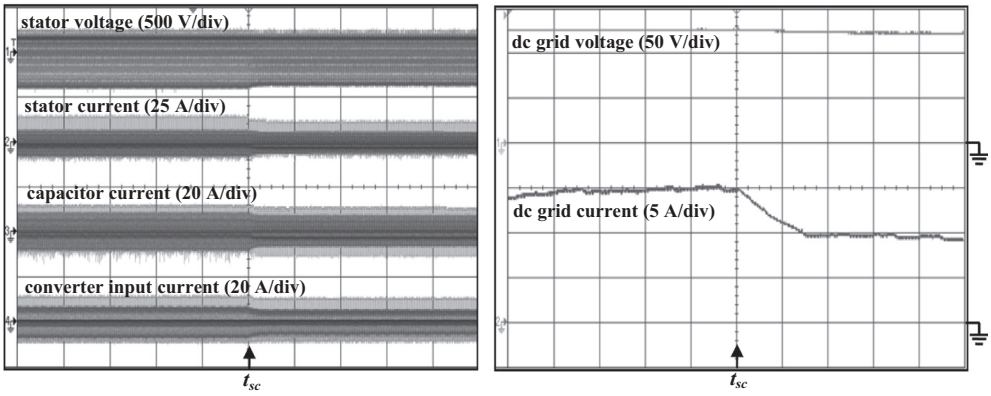

Fig. 8. Dynamic response of the MPPT for step change in rotor speed from 1350 to 1250 rpm, C = 100 μF/phase, V_{dc} = 120 V and t_{sc}: instant at which rotor speed change is initiated. Time axis: 2 s/div.

Fig. 9. Photograph of experimental setup.

3.92 kW for a rotor speed of 1500 rpm with 100-μF excitation capacitor per phase. The maximum value of SEIG output power will reduce as the speed decreases for the same excitation capacitance. This aspect i.e., step change in the speed has been used for showing the dynamic response of the proposed MPPT controller in the laboratory. One such experimental result is given in Fig. 8 for change in the speed from 1350 to 1250 rpm. This experimental result further confirms the successful working of the proposed WECS and MPPT controller for dc microgrid application. Fig. 9 shows the photograph of the experimental set-up of the proposed WECS.

5. Conclusion

This paper has proposed a wind-driven SEIG with a single-stage power converter for supplying/feeding dc microgrid. A simple MPPT algorithm, which constantly monitors the dc grid current and adjusts the firing angle of the three-phase semi-converter, for extracting MP available in the wind has been proposed. This MPPT algorithm does not depend on the machine parameters and actual wind velocity or WT rotor speed and hence it is simple to implement. Thus, the single power electronic converter stage and parameter insensitive MPPT algorithm are the attractive features of the proposed WECS supplying to dc microgrid. A MATLAB/Simulink model has been developed for analyzing the steady-state and dynamic performance of the proposed system. The results obtained on this simulation model show that the proposed MPPT algorithm clearly tracks the MP available in the wind by operating the WT at specific rotor speed/mechanical output power for a given wind velocity.

The efficacy and successful working of the proposed system has also been demonstrated with the help of an experimental prototype model developed using a 3-phase, 3.7 kW SEIG system. Thyristor based semi-converter along with the ZCD and pulse-triggering circuits has also been built as part of this experimental set-up. The closed-loop control algorithm has been implemented using dsPIC30F4011 DSC for this experimental study. Experimental results obtained on the prototype model agree closely with the values obtained using simulation model for various operating conditions. This validates the analysis of the system through the simulation developed in the paper. It is to be noted that the present system will have the current harmonics at the generator terminals and hence an appropriate filter is essential for operating the SEIG to its rated value.

Acknowledgment

Authors wish to thank the authorities of the National Institute of Technology, Tiruchirappalli, India for all the facilities provided for carrying out the experimental and simulation work for the preparation of this paper.

References

[1] Global Wind Energy Council, Global Wind Power Statistics, 2015. <http://www.gwec.net/global-figures/graphs> (accessed on 29.04.16).
[2] A.R. Sudhamshu, M.C. Pandey, N. Sunil, N.S. Satish, V. Mugundhan, R.K. Velamati, Numerical study of effect of pitch angle on performance characteristics of a HAWT, Int. J. Eng. Sci. Technol. 19 (1) (2016) 632–641.
[3] H. Li, Z. Chen, Overview of different wind generator systems and their comparisons, IET Renew. Power Gener. 2 (2) (2008) 123–138.
[4] Q. Wang, L. Chang, An intelligent maximum power extraction algorithm for inverter-based variable speed wind turbine systems, IEEE Trans. Power Electron. 19 (5) (2004) 1242–1249.
[5] P. Raja, N. Kumaresan, M. Subbiah, Grid-connected induction generators using delta-star switching of the stator winding with a permanently connected capacitor, Int. J. Wind Eng. 36 (2) (2012) 219–232.
[6] B. Singh, S.S. Murthy, R.S. Reddy, P. Arora, Implementation of modified current synchronous detection method for voltage control of self-excited induction generator, IET Power Electron. 8 (7) (2015) 1146–1155.
[7] R.R. Chilipi, B. Singh, S.S. Murthy, Performance of a self-excited induction generator with DSTATCOM-DTC drive-based voltage and frequency controller, IEEE Trans. Energy Convers. 29 (3) (2014) 545–557.
[8] S. Senthil Kumar, N. Kumaresan, M. Subbiah, M. Rageeru, Modelling, analysis and control of stand-alone self-excited induction generator-pulse width modulation rectifier systems feeding constant DC voltage applications, IET Gener. Transm. Distrib. 8 (6) (2014) 1140–1155.
[9] A. Kheldoun, L. Refoufi, D.E. Khodja, Analysis of the self-excited induction generator steady state performance using a new efficient algorithm, Electric Power Syst. Res. 86 (2012) 61–67.
[10] R. Karthigaivel, N. Kumaresan, M. Subbiah, Analysis and control of self-excited induction generator-converter systems for battery charging applications, IET Electric Power Appl. 5 (2) (2011) 247–257.
[11] D. Joshi, K.S. Sandhu, M.K. Soni, Constant voltage constant frequency operation for a self-excited induction generator, IEEE Trans. Energy Convers. 21 (1) (2006) 228–234.
[12] N. Ammasaigounden, M. Subbiah, Microprocessor-based voltage controller for wind-driven induction generators, IEEE Trans. Ind. Electron. 37 (6) (1990) 531–537.
[13] S. Senthil Kumar, N. Kumaresan, M. Subbiah, Analysis and control of capacitor-excited induction generators connected to a micro-grid through power electronic converters, IET Gener. Transm. Distrib. 9 (10) (2015) 911–920.
[14] S. Senthil Kumar, N. Kumaresan, N. Ammasai Gounden, Namani Rakesh, Analysis and control of wind-driven self-excited induction generators connected to the grid through power converters, Front Energy 6 (4) (2012) 403–412.
[15] K. Nishida, T. Ahmed, M. Nakaoka, A cost-effective high-efficiency power conditioner with simple MPPT control algorithm for wind-power grid integration, IEEE Trans. Ind. Appl. 47 (2) (2011) 893–900.
[16] V. Agarwal, R.K. Aggarwal, P. Patidar, C. Patki, A novel scheme for rapid tracking of maximum power point in wind energy generation systems, IEEE Trans. Energy Convers. 25 (1) (2010) 228–236.
[17] Z. Chen, J.M. Guerrero, F. Blaabjerg, A review of the state of the art of power electronics for wind turbines, IEEE Trans. Power Electron. 24 (8) (2009) 1859–1875.
[18] B.C. Babu, K. Sridharan, E. Rosolowski, Z. Leonowicz, Analysis of SDFT based phase detection system for grid synchronization of distributed generation systems, Int. J. Eng. Sci. Technol. 17 (2014) 270–278.
[19] Z. Chen, E. Spooner, Grid power quality with variable speed wind turbines, IEEE Trans. Energy Convers. 16 (2) (2001) 148–154.
[20] N. Kumar, T.R. Chelliah, S.P. Srivastava, Analysis of doubly-fed induction machine operating at motoring mode subjected to voltage sag, Int. J. Eng. Sci. Technol. (2016), http://dx.doi.org/10.1016/j.jestch.2016.01.015.
[21] K. Vijayakumar, N. Kumaresan, N. Ammasai Gounden, S.B. Tennakoon, Real and reactive power control of hybrid excited wind-driven grid-connected doubly fed induction generators, IET Power Electron. 6 (6) (2013) 1197–1208.
[22] M.-S. Lu, C.-L. Chang, W.-J. Lee, L. Wang, Combining the wind power generation system with energy storage equipment, IEEE Trans. Ind. Appl. 45 (6) (2009) 2109–2115.
[23] J.P. Barton, D.G. Infield, Energy storage and its use with intermittent renewable energy, IEEE Trans. Energy Convers. 19 (2) (2004) 441–448.
[24] P. Wang, L. Goel, X. Liu, F.H. Choo, Harmonizing AC and DC: a hybrid AC/DC future grid solution, IEEE Power Energy Mag. 11 (3) (2013) 76–83.
[25] J.J. Justo, F. Mwasilu, J. Lee, J.-W. Jung, AC-microgrids versus DC-microgrids with distributed energy resources: a review, Renew. Sustain. Energy Rev. 24 (2013) 387–405.
[26] D. Das, N. Kumaresan, V. Nayanar, K. Navin Sam, N. Ammasai Gounden, Development of BLDC motor based elevator system suitable for DC microgrid, IEEE/ASME Trans. Mechatron. 21 (3) (2016) 1552–1560.
[27] G. Byeon, T. Yoon, S. Oh, G. Jang, Energy management strategy of the dc distribution system in buildings using the EV service model, IEEE Trans. Power Electron. 28 (4) (2013) 1544–1554.
[28] L. Xu, D. Chen, Control and operation of a DC microgrid with variable generation and energy storage, IEEE Trans. Power Del. 26 (4) (2011) 2513–2522.
[29] W. Li, X. Mou, Y. Zhou, C. Marnay, On voltage standards for DC home microgrids energized by distributed sources, in: Proceeding 7th International Power Electronics and Motion Control Conference (IPEMC'12), Harbin, China, 2012, pp. 2282–2286.
[30] S. Anand, B.G. Fernandes, Optimal voltage level for DC microgrids, in: Proceeding 36th Annual Conference on IEEE Industrial Electronics Society (IECON'10), Glendale, AZ, 2010, pp. 3034–3039.
[31] K. Strunz, E. Abbasi, D.N. Huu, DC microgrid for wind and solar power integration, IEEE, J. Emerg. Sel. Top. Power Electron. 2 (1) (2014) 115–126.
[32] V. Nayanar, N. Kumaresan, N. Ammasai Gounden, A single sensor based MPPT controller for wind-driven induction generators supplying DC microgrid, IEEE Trans. Power Electron. 31 (2) (2016) 1161–1172.